Frontiers of Information Technology & Electronic Engineering
www.jzus.zju.edu.cn; engineering.cae.cn; www.springerlink.com
ISSN 2095-9184 (print); ISSN 2095-9230 (online)
E-mail: jzus@zju.edu.cn

Adaptive robust neural control of a two-manipulator system holding a rigid object with inaccurate base frame parameters*

Fan XU, Jin WANG[†‡], Guo-dong LU

State Key Laboratory of Fluid Power and Mechatronic Systems, Zhejiang University, Hangzhou 310027, China

[†]E-mail: dwjcom@zju.edu.cn

Received Nov. 16, 2016; Revision accepted Apr. 17, 2017; Crosschecked Nov. 27, 2018

Abstract: The problem of self-tuning control with a two-manipulator system holding a rigid object in the presence of inaccurate translational base frame parameters is addressed. An adaptive robust neural controller is proposed to cope with inaccurate translational base frame parameters, internal force, modeling uncertainties, joint friction, and external disturbances. A radial basis function neural network is adopted for all kinds of dynamical estimation, including undesired internal force. To validate the effectiveness of the proposed approach, together with simulation studies and analysis, the position tracking errors are shown to asymptotically converge to zero, and the internal force can be maintained in a steady range. Using an adaptive engine, this approach permits accurate online calibration of the relative translational base frame parameters of the involved manipulators. Specialized robust compensation is established for global stability. Using a Lyapunov approach, the controller is proved robust in the face of inaccurate base frame parameters and the aforementioned uncertainties.

Key words: Cooperative manipulators; Neural networks; Inaccurate translational base frame; Adaptive control; Robust control
https://doi.org/10.1631/FITEE.1601707 **CLC number:** TP241.2

1 Introduction

In many modern manufacturing applications, such as material handling, grasping, and transporting, it is necessary to move a large and heavy payload using cooperative manipulators that must share the load and provide stiffness. Consider that certain kinematic and dynamic constraints will be formed because the manipulators have to remain in contact with the object while in motion, which may lead to undesired stress. It is much more complicated to design a controller of cooperative manipulation. All the manipulators have to move synchronously to track a certain desired position and orientation leading to further complex internal forces, while those internal forces contribute nothing to the motion of the object. Experiments have shown that even small kinematic inaccuracy can significantly affect the tracking performance (Aghili, 2013), among which base frame parameters are usually difficult to obtain and are thus ignored. Such cooperative manipulator systems should be robust enough against these effects resulting from inaccurate translational base frame parameters, internal forces, common model uncertainty, joint frictions, and external disturbances.

Various studies of cooperative manipulators are mostly based on the knowledge of system dynamics with non-adaptive or adaptive mechanisms. A distributed impedance controller (Szewczyk et al., 2002) was developed based on a realistic model including robot and object dynamics. Using a switching-sliding algorithm, a robust controller (Liu and Abdel-Malek, 2000) was proposed for modeling imprecision and disturbances in the presence of contact and friction

‡ Corresponding author

* Project supported by the National Natural Science Foundation of China (No. 51675470), the National Key R&D Program of China (No. 2017YFB1301203), and the Fundamental Research Funds for the Central Universities, China (No. 2017QNA4001)

ORCID: Jin WANG, https://orcid.org/0000-0003-3106-021X

constraints for grasping conditions. When system uncertainties and external disturbances are considered in practical applications, many adaptive control schemes have been proposed (Su and Stepanenko, 1995; Parra-Vega et al., 2003; Namvar and Aghili, 2005; Gueaieb et al., 2007b; Tavasoli et al., 2009); however, these schemes estimate system physical parameters that require certain knowledge of dynamics, extensive preliminary system modeling, or regression computing during operation. Neural network (NN) algorithms have shown an outstanding ability in compensating for uncertainties and developing dynamic model-free controllers. Panwar et al. (2012) developed an adaptive neural controller for cooperative manipulation of a rigid object, where no preliminary learning was required, but internal force feedback was required. A radial basis function (RBF) NN enhanced estimator and observer were developed (Zhao et al., 2014b, 2014c) to estimate acceleration and control torque online, but they were designed only for leader-follower manipulator system circumstances.

Although these adaptive control schemes can deal with dynamic uncertainties of cooperative manipulator systems, the closed kinematic chain of interconnected cooperation is assumed to be precisely known. In the presence of uncertain kinematics, an adaptive synchronized tracking control approach was developed (Zhao et al., 2014a) using a cross-coupling technique, but for non-closed-loop circumstances with no robotic cooperation. An adaptive strategy was developed by Lizarralde et al. (2013), addressing the visual tracking problem of robot manipulators with non-negligible dynamics using a fixed camera, when the camera-robot system parameters were uncertain. Cheng et al. (2009) proposed an NN-based adaptive controller where a 'linearity-in-parameters' assumption for the uncertain terms was unnecessary. Mohajerpoor et al. (2011) presented a robust hybrid force/position control scheme of two cooperative manipulators handling an unknown object interacting with an unknown environment, but with known manipulator dynamics. A hybrid task-space trajectory and force tracking based on a fuzzy system and adaptive mechanism (Li et al., 2015) was proposed to compensate for external perturbation, kinematics, and dynamics uncertainties. Liu (2015) designed adaptive controllers for a network of heterogeneous robots to achieve task-space synchronization in the presence of uncertainties in kinematic and dynamic models, based on which networked robot systems could be ensured to synchronize with imprecise measurement of system parameters and communication delays. Other control algorithms and adaptive laws were developed (Liu and Khong, 2015) to address the impediment of imprecise measurement resulting from an unknown grasping point and orientation.

The base frame parameters, which determine the relative translation and rotation between base frames of the coordinated manipulators, present a fundamental kinematic problem for coordinated cooperative manipulator systems (Corke, 1996). With respect to negligible robotic manufacturing and assembling kinematic errors, the inaccurate base frame calibration contributes more obviously to interference. There exist some studies on multirobot base frame calibration (Gan and Dai, 2011; Zhang et al., 2011; Deng et al., 2015); however, precision end-point or camera-based measurement systems are required to calibrate the relative kinematic parameters of the manipulators (Park et al., 2012). Aghili (2011, 2013) proposed several self-tuning cooperative manipulator controllers to track motion trajectory without knowing the true kinematic parameters, and at the same time permit accurate calibration of the relative base frame parameters of the involved manipulators. Though there is no need for high-precision end-point sensing or force measurements, the internal force is hardly managed.

In a brief summary of the control approaches in the literature, some scholars have done much research work, but there are still some issues that require improvement: (1) inaccurate base frame parameters (the base frame affects the closed kinematic chain directly, but most control algorithms have seldom considered inaccurate base frame parameters); (2) internal force (permanent damage to an object may occur with unmanaged internal force, but most of the existing coordinated control methods ignore internal force or require specific force sensors); (3) uncertain dynamics, joint frictions, and the external disturbances (for most cooperating controllers, dynamic knowledge of manipulators and environment is more or less necessary, which is always practically out of reach).

2 Preparation problem formulation and preliminaries

Fig. 1 illustrates two cooperative manipulators. Each manipulator holds a common rigid object at specified points. Coordinate frames $\boldsymbol{c}_{\mathrm{w}}$, $\boldsymbol{c}_1$, and $\boldsymbol{c}_2$ are attached to the world origin and end effectors of the manipulators, respectively. The coordinate frame $\boldsymbol{c}_{\mathrm{o}}$ is assumed to be located in the geometric center of the object and its principal axis coincides with the connecting line of the end effectors, i.e., $\boldsymbol{c}_{\mathrm{o}}=(\boldsymbol{c}_1-\boldsymbol{c}_2)/\|\boldsymbol{c}_1-\boldsymbol{c}_2\|$. Throughout this paper, all quantities are expressed with reference to the self-defined world frame.

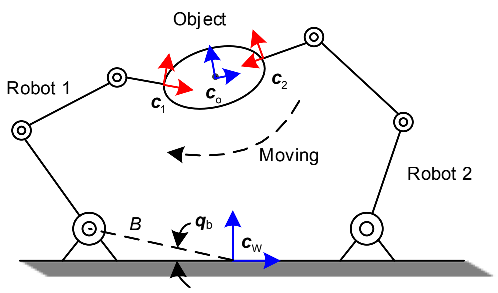

Fig. 1 Two cooperative manipulators holding a rigid object

Assumption 1 The object is rigidly grasped by the end effectors, such that there is no relative translational motion between the end effectors and the object.

Assumption 2 Consider that calibration equipment is expensive and that some bases are defined inside the manipulators (usually as the first two axis joints), and the relative positions of the manipulators' base frames are not precisely obtained. In the following, we focus on the translational base frame parameters, such that the manipulators' forward kinematics are supposed to be precisely known.

All cooperative manipulators must be controlled synchronously and carefully to move the object and ensure that its center of mass tracks on a predefined trajectory under an inaccurate relative translational base frame, existing joint frictions, and other unknown external disturbances.

2.1 Kinematics

Let $\boldsymbol{x}$ denote the task space vector of the object, including its position and orientation. The forward kinematics $\boldsymbol{x}_i$ for manipulator i can be written as

$$\boldsymbol{x}_i=\phi_i(\boldsymbol{q}_i),\ \ i=1,2,\ldots,m, \tag{1}$$

$$\dot{\boldsymbol{x}}_i=\dot{\phi}_i(\boldsymbol{q}_i)=\boldsymbol{J}_i\dot{\boldsymbol{q}}_i,\ i=1,2,\ldots,m, \tag{2}$$

where $\boldsymbol{q}_i$ represents joint coordinates, and $\boldsymbol{J}_i$ is the Jacobian matrix from the joint space to the task space.

Considering the inaccurate relative base frame worldwide (Fig. 1), we set additional $\boldsymbol{q}_{\mathrm{b}i}$ and $\boldsymbol{B}_i$ for orientation of the base joint and inaccurate translational base frame, respectively. We consider translational base frame parameters as part of the robotic kinematic parameters. Hence, with traditional joint coordinates $\boldsymbol{q}_i$ and constant kinematic parameters $\boldsymbol{\theta}_{\mathrm{k}i}$, a new set of $\bar{\boldsymbol{q}}_i=[\boldsymbol{q}_{\mathrm{b}i},\boldsymbol{q}_i]^{\mathrm{T}}$ and $\hat{\boldsymbol{\theta}}_{\boldsymbol{B}i}=[\hat{\boldsymbol{B}}_i,\boldsymbol{\theta}_{\mathrm{k}i}]^{\mathrm{T}}$ is designed, and then we have

$$\hat{\boldsymbol{x}}_i=\hat{\phi}_i(\bar{\boldsymbol{q}}_i)=\boldsymbol{Y}(\bar{\boldsymbol{q}}_i)\hat{\boldsymbol{\theta}}_{\boldsymbol{B}i}, \tag{3}$$

$$\dot{\hat{\boldsymbol{x}}}_i=\hat{\boldsymbol{J}}_i\dot{\bar{\boldsymbol{q}}}_i=\boldsymbol{Y}_{\mathrm{k}}(\bar{\boldsymbol{q}}_i,\dot{\bar{\boldsymbol{q}}}_i)\hat{\boldsymbol{\theta}}_{\boldsymbol{B}i}, \tag{4}$$

where $\boldsymbol{Y}(\bar{\boldsymbol{q}}_i)$ and $\boldsymbol{Y}_{\mathrm{k}i}$ (short for $\boldsymbol{Y}_{\mathrm{k}}(\bar{\boldsymbol{q}}_i,\dot{\bar{\boldsymbol{q}}}_i)$) are the corresponding kinematic regression matrices. '$\hat{*}$' stands for an estimated term of *, and '$\tilde{*}$' denotes the relevant estimation error. Then we have kinematic estimation error $\tilde{\boldsymbol{\theta}}_{\boldsymbol{B}i}=\boldsymbol{\theta}_{\boldsymbol{B}i}-\hat{\boldsymbol{\theta}}_{\boldsymbol{B}i}$.

Assumption 3 We assume that the manipulators move in a finite task space such that the Jacobian matrices and their estimates are of full rank.

Assumption 4 We focus on inaccurate translational parameter $\boldsymbol{B}_i$, which means that the base frame parameters here include inaccuracies along both vertical and horizontal axes.

2.2 Dynamics

The dynamic equation of the i^{th} manipulator with n_i joints in the cooperative system is similar to that in Gueaieb et al. (2007b):

$$\widehat{\boldsymbol{D}}_i\ddot{\boldsymbol{q}}_i+\widehat{\boldsymbol{C}}_i\dot{\boldsymbol{q}}_i+\widehat{\boldsymbol{G}}_i-(\boldsymbol{\tau}_{\mathrm{f}_i}(\dot{\boldsymbol{q}}_i)+\boldsymbol{d}_i(t))=\boldsymbol{\tau}_i+\boldsymbol{J}_i^{\mathrm{T}}\boldsymbol{f}_i, \tag{5}$$

where

$$\begin{aligned}
&\widehat{\boldsymbol{D}}_i=\boldsymbol{M}_i(\boldsymbol{q}_i)+\boldsymbol{\varpi}_i(t)\boldsymbol{M}_{\mathrm{o}}(\boldsymbol{q}_i),\\
&\widehat{\boldsymbol{C}}_i=\boldsymbol{Q}_i(\boldsymbol{q}_i,\dot{\boldsymbol{q}}_i)+\boldsymbol{\varpi}_i(t)[\boldsymbol{J}_i^{\mathrm{T}}\boldsymbol{M}_{\mathrm{o}}(x)\dot{\boldsymbol{J}}_i+\boldsymbol{Q}_{\mathrm{o}}(\boldsymbol{q}_i,\dot{\boldsymbol{q}}_i)],\\
&\widehat{\boldsymbol{G}}_i=\boldsymbol{W}_i(\boldsymbol{q}_i)+\boldsymbol{\varpi}_i(t)\boldsymbol{W}_{\mathrm{o}}(\boldsymbol{q}_i),\\
&\boldsymbol{M}_{\mathrm{o}}(\boldsymbol{q}_i)=\boldsymbol{J}_i^{\mathrm{T}}\boldsymbol{M}_{\mathrm{o}}(x)\boldsymbol{J}_i,
\end{aligned}$$

$$\boldsymbol{Q}_{\mathrm{o}}(\boldsymbol{q}_i,\dot{\boldsymbol{q}}_i)=\boldsymbol{J}_i^{\mathrm{T}}\boldsymbol{Q}_{\mathrm{o}}(\boldsymbol{x},\dot{\boldsymbol{x}})\boldsymbol{J}_i,$$
$$\boldsymbol{W}_{\mathrm{o}}(\boldsymbol{q}_i)=\boldsymbol{J}_i^{\mathrm{T}}\boldsymbol{W}_{\mathrm{o}}(\boldsymbol{x}),$$

where $\boldsymbol{\tau}_i$ denotes the joint torque/force applied by the actuators on the i^{th} manipulator, $\boldsymbol{M}_i(\dot{\boldsymbol{q}}_i)$ and $\boldsymbol{M}_{\mathrm{o}}(\boldsymbol{x})$ denote the inertial matrices, with subscripts 'i' and 'o' standing for the i^{th} manipulator and the object, respectively, $\boldsymbol{Q}_i(\boldsymbol{q}_i,\dot{\boldsymbol{q}}_i)$ and $\boldsymbol{Q}_{\mathrm{o}}(\boldsymbol{x},\dot{\boldsymbol{x}})$ are the Coriolis and centrifugal matrices, respectively, $\boldsymbol{W}_i(\boldsymbol{q}_i)$ and $\boldsymbol{W}_{\mathrm{o}}(\boldsymbol{x})$ represent the vectors of gravitational forces, $\boldsymbol{\tau}_{\mathrm{f}_i}(\dot{\boldsymbol{q}}_i)$ stands for the joint friction, $\boldsymbol{d}_i(t)$ is an unknown external disturbance, $\boldsymbol{f}_i$ denotes the internal force, and $\boldsymbol{\varpi}_i(t)$ is considered a time-independent positive-definite diagonal matrix representing the load distribution of the object on the i^{th} manipulator. The following property is important:

Property 1 Unlike Gueaieb et al. (2007b), the matrix $2\widehat{\boldsymbol{C}}_i-\dot{\widehat{\boldsymbol{D}}}_i+\dot{\boldsymbol{\varpi}}_i\boldsymbol{J}_i^{\mathrm{T}}\boldsymbol{M}_{\mathrm{o}}(\boldsymbol{x})\boldsymbol{J}_i$ is a skew symmetric matrix, and hence $\boldsymbol{p}^{\mathrm{T}}(2\widehat{\boldsymbol{C}}_i-\dot{\widehat{\boldsymbol{D}}}_i+\dot{\boldsymbol{\varpi}}_i\boldsymbol{J}_i^{\mathrm{T}}\boldsymbol{M}_{\mathrm{o}}(\boldsymbol{x})\boldsymbol{J}_i)\boldsymbol{p}$ =0 for $\boldsymbol{p}\in\mathbb{R}^{n_i}$.

2.3 Radial basis function neural network

The RBF NN has some satisfactory features such as weight adjustment and mathematical tractability, and it is widely used in cooperative manipulating controller design (Panwar et al., 2012; Zhao et al., 2014b, 2014c). The output vector $\boldsymbol{h}(\boldsymbol{\Xi})$ of an RBF NN with hn units in the hidden layer is determined in terms of the input vector $\boldsymbol{\Xi}$ by the following mapping:

$$\boldsymbol{h}(\boldsymbol{\Xi})=\boldsymbol{\Theta}^{\mathrm{T}}\boldsymbol{\psi}(\boldsymbol{\Xi}),\tag{6}$$

where $\boldsymbol{\psi}(\boldsymbol{\Xi})$ are the outputs of the hidden layer, with

$$\boldsymbol{\psi}(\boldsymbol{\Xi})=[\theta_1,\theta_2,\cdots,\theta_{hn}],\tag{7}$$
$$\theta_i=\exp\left(-\|\boldsymbol{\Xi}-\boldsymbol{c}_i\|^2/b_i^2\right),\tag{8}$$

where $\boldsymbol{c}_i$ is the center and b_i is the width of the kernel unit. Each kernel node in the RBF NN provides an output, which depends on a radially symmetric function, and a better performance will be achieved when the input is near the centroid. In the following assumption, the RBF NN shows an arbitrary precision approach capability in a compact set range for a continuous function (Park and Sandberg, 1991).

Assumption 5 The NN output is continuous, and for the object term $\boldsymbol{\Lambda}$ there exists an ideal NN approach of NN, for a very small positive number ε_0:

$$\max\|\boldsymbol{h}(\boldsymbol{\Xi})-\boldsymbol{\Lambda}\|\le\varepsilon_0,\tag{9}$$

where $\tilde{\boldsymbol{h}}(\boldsymbol{\Xi})=\boldsymbol{h}(\boldsymbol{\Xi})-\hat{\boldsymbol{h}}(\boldsymbol{\Xi})$ is the approximation error of NN, and $\hat{\boldsymbol{h}}(\boldsymbol{\Xi})$, defined as the estimate of $\boldsymbol{h}(\boldsymbol{\Xi})$, can be given by

$$\hat{\boldsymbol{h}}(\boldsymbol{\Xi})=\hat{\boldsymbol{\Theta}}^{\mathrm{T}}\boldsymbol{\psi}(\boldsymbol{\Xi}),\tag{10}$$

where $\hat{\boldsymbol{\Theta}}$ estimates the ideal NN weights provided by online tuning algorithms, with corresponding weight estimation error $\tilde{\boldsymbol{\Theta}}$.

3 Design of adaptive neural robust controller

In this section, we present an adaptive neural network robust (ANNR) controller for cooperative manipulators with inaccurate translational base frames, unknown joint friction, and external disturbances. We define the task space position error of the object:

$$\boldsymbol{e}=\boldsymbol{x}-\boldsymbol{x}_{\mathrm{d}},\tag{11}$$

where subscript 'd' stands for the desired term. The distance of the task space coordinates among the manipulators should be a constant during movement, such that internal force can be prevented. This can be mapped by an estimated synchronization function for the two manipulators:

$$\boldsymbol{e}_{\mathrm{s}1}=-\boldsymbol{e}_{\mathrm{s}2}=\hat{\boldsymbol{x}}_1-\hat{\boldsymbol{x}}_2.\tag{12}$$

To describe the relative motion among the coordinated manipulators, the following task space cross-coupling error is defined:

$$\varsigma_i=\boldsymbol{e}+\beta\left(\boldsymbol{e}_{\mathrm{s}i}+\boldsymbol{K}_{\mathrm{I}}\int_0^t\boldsymbol{e}(\omega)\mathrm{d}\omega\right),\tag{13}$$

with a control coefficient taken as

$$\dot{\boldsymbol{x}}_{\mathrm{r}i}=\dot{\boldsymbol{x}}_{\mathrm{d}}-\alpha\boldsymbol{\varsigma}_i, \tag{14}$$

where β and α are positive constants and $\boldsymbol{K}_{\mathrm{I}}$ is a positive-definite diagonal integration matrix. Similar to Cheah et al. (2004), we define an adaptive task space sliding vector as

$$\boldsymbol{s}_{xi}=\dot{\hat{\boldsymbol{x}}}_i-\dot{\boldsymbol{x}}_{\mathrm{r}i}, \tag{15}$$

and hence we have an adaptive sliding vector in the joint space defined as

$$\boldsymbol{s}_i=\dot{\boldsymbol{q}}_i-\dot{\boldsymbol{q}}_{\mathrm{r}i}=\hat{\boldsymbol{J}}_i^{+}\boldsymbol{s}_{xi}, \tag{16}$$

where $\dot{\boldsymbol{q}}_{\mathrm{r}i}=\hat{\boldsymbol{J}}_i^{+}\dot{\boldsymbol{x}}_{\mathrm{r}i}$ indicates the control coefficient in the joint space, and $\hat{\boldsymbol{J}}_i^{+}=\hat{\boldsymbol{J}}_i^{\mathrm{T}}(\hat{\boldsymbol{J}}_i\hat{\boldsymbol{J}}_i^{\mathrm{T}})^{-1}$ is the pseudo-inverse of the estimated Jacobian matrix. According to Eq. (24) in Erhart and Hirche (2013), we can infer that the cooperative internal force here can be expressed in the form:

$$\boldsymbol{f}_i=\boldsymbol{f}_i\left(\boldsymbol{c}_{\mathrm{o}},\boldsymbol{c}_1,\boldsymbol{c}_2,\dot{\boldsymbol{x}}\right). \tag{17}$$

Considering the preliminaries and using the forward kinematic relationships, Eq. (17) can be rewritten as

$$\boldsymbol{f}_i=\boldsymbol{f}_i\left(\boldsymbol{p}_{\mathrm{e}1},\boldsymbol{p}_{\mathrm{e}2},\boldsymbol{e}_{\mathrm{s}i},\dot{\boldsymbol{x}}\right)=\boldsymbol{f}_i\left(\boldsymbol{q}_1,\boldsymbol{q}_2,\boldsymbol{e}_{\mathrm{s}i},\dot{\boldsymbol{x}},\hat{\boldsymbol{\theta}}_{\boldsymbol{B}i}\right), \tag{18}$$

where $\boldsymbol{p}_{\mathrm{e}1}$ and $\boldsymbol{p}_{\mathrm{e}2}$ denote the positions of each manipulator's end effector. Substituting Eq. (16) into the system dynamics (5), we obtain the filtered tracking error as

$$\widehat{\boldsymbol{D}}_i\dot{\boldsymbol{s}}_i=-\left[\widehat{\boldsymbol{D}}_i\ddot{\boldsymbol{q}}_{\mathrm{r}i}+\widehat{\boldsymbol{C}}_i\dot{\boldsymbol{q}}_{\mathrm{r}i}+\widehat{\boldsymbol{G}}_i-\boldsymbol{J}_i^{\mathrm{T}}\boldsymbol{f}_i\right]-\widehat{\boldsymbol{C}}_i\boldsymbol{s}_i+\boldsymbol{\tau}_{d_i}+\boldsymbol{\tau}_i, \tag{19}$$

where $\boldsymbol{\tau}_{d_i}=\boldsymbol{\tau}_{f_i}(\dot{\boldsymbol{q}}_i)+\boldsymbol{d}_i(t)$. Using an RBF NN $\boldsymbol{h}_i(\boldsymbol{\varXi}_i)$, we can obtain

$$\begin{aligned}\boldsymbol{\varLambda}_i&=\widehat{\boldsymbol{D}}_i(\boldsymbol{q}_i,\boldsymbol{J}_i,\boldsymbol{x})\ddot{\boldsymbol{q}}_{\mathrm{r}i}+\widehat{\boldsymbol{C}}_i(\boldsymbol{q}_i,\dot{\boldsymbol{q}}_i,\boldsymbol{J}_i,\boldsymbol{x})\dot{\boldsymbol{q}}_{\mathrm{r}i}\\&\quad+\widehat{\boldsymbol{G}}_i(\boldsymbol{q}_i,\boldsymbol{J}_i,\boldsymbol{x})-\boldsymbol{J}_i^{\mathrm{T}}\boldsymbol{f}_i\left(\boldsymbol{q}_1,\boldsymbol{q}_2,\boldsymbol{e}_{\mathrm{s}i},\dot{\boldsymbol{x}},\hat{\boldsymbol{\theta}}_{\boldsymbol{B}i}\right)\\&=\boldsymbol{h}_i(\boldsymbol{\varXi}_i)+\boldsymbol{\varepsilon}_i,\end{aligned} \tag{20}$$

where $\boldsymbol{\varXi}_i$ can be chosen as $\boldsymbol{\varXi}_i=[\boldsymbol{q}_i,\dot{\boldsymbol{q}}_i,\boldsymbol{x}_{\mathrm{d}},\dot{\boldsymbol{x}}_{\mathrm{d}},\ddot{\boldsymbol{x}}_{\mathrm{d}},\boldsymbol{e}_{\mathrm{s}i},\hat{\boldsymbol{\theta}}_{\boldsymbol{B}i}]$ and $\boldsymbol{\varepsilon}_i$ is the NN functional approximation error. Based on the aforementioned design, the adaptive robust neural control scheme is proposed in the following form:

$$\boldsymbol{\tau}_i=\hat{\boldsymbol{h}}_i(\boldsymbol{\varXi})-\hat{\boldsymbol{J}}_i^{\mathrm{T}}\boldsymbol{E}_i-\boldsymbol{w}_{1i}\boldsymbol{E}_i+\boldsymbol{w}_{2i}, \tag{21}$$

where $\hat{\boldsymbol{h}}_i(\boldsymbol{\varXi}_i)=\hat{\boldsymbol{\Theta}}_i^{\mathrm{T}}\boldsymbol{\psi}(\boldsymbol{\varXi}_i)$ is the estimation term of the system nonlinear function $\boldsymbol{\varLambda}_i$, $\boldsymbol{E}_i=\boldsymbol{K}_{\mathrm{V}}\dot{\boldsymbol{\varsigma}}_i+\boldsymbol{K}_{\mathrm{P}}\boldsymbol{\varsigma}_i$ with positive-definite diagonal matrices $\boldsymbol{K}_{\mathrm{V}}$ and $\boldsymbol{K}_{\mathrm{P}}$, and w_{1i} and w_{2i} are the robust adaptive term and the robust estimation term of the network, respectively, given by

$$\boldsymbol{w}_{1i}=(\boldsymbol{s}_i^{\mathrm{T}})^{+}\left(\beta\dot{\boldsymbol{e}}_{\mathrm{s}i}^{\mathrm{T}}+\beta\boldsymbol{K}_{\mathrm{I}}\boldsymbol{e}^{\mathrm{T}}\right), \tag{22}$$

$$\boldsymbol{w}_{2i}=-b_0\left\|\hat{\boldsymbol{\Theta}}\right\|_{\mathrm{F}}\left\|\boldsymbol{Y}_{\mathrm{b}}^{\mathrm{T}}\dot{\boldsymbol{e}}_{\mathrm{s}i}\right\|\mathrm{sgn}(\boldsymbol{s}_i)-b_1\left\|\boldsymbol{s}_i^{\mathrm{T}}\right\|\mathrm{sgn}(\boldsymbol{s}_i), \tag{23}$$

where β, b_0, and b_1 are positive constants, and $\|*\|_{\mathrm{F}}$ stands for the Frobenius norm. To guarantee the convergence of the position error and to make it converge in a synchronous manner, the terms $\boldsymbol{e}^{\mathrm{T}}$ and $\dot{\boldsymbol{e}}_{\mathrm{s}i}^{\mathrm{T}}$ are both adopted in w_{1i}. Considering both dynamic and kinematic estimation errors, we use a combination as $\left\|\hat{\boldsymbol{\Theta}}\right\|_{\mathrm{F}}\left\|\boldsymbol{Y}_{\mathrm{b}}^{\mathrm{T}}\dot{\boldsymbol{e}}_{\mathrm{s}i}\right\|\mathrm{sgn}(\boldsymbol{s}_i)$ for estimation robustness. Furthermore, joint frictions and external disturbances are handled by a common $\left\|\boldsymbol{s}_i^{\mathrm{T}}\right\|\mathrm{sgn}(\boldsymbol{s}_i)$ design, to achieve overall robustness. $\boldsymbol{Y}_{\mathrm{b}}^{\mathrm{T}}\dot{\boldsymbol{e}}_{\mathrm{s}i}$ maintains the component of $\dot{\boldsymbol{e}}_{\mathrm{s}i}$ with a gain according to the inaccurate translational base frame (here as X- and Y-axis component for simplicity), which means that the base frame parameters here are inaccurate along both the X- and Y-axis. The adaptive NN control rule can be selected as

$$\dot{\hat{\boldsymbol{\Theta}}}_i=-\eta\left(\boldsymbol{\psi}(\boldsymbol{\varXi}_i)\boldsymbol{s}_i^{\mathrm{T}}+\left\|\boldsymbol{s}_i^{\mathrm{T}}\right\|\hat{\boldsymbol{\Theta}}_i+\left\|\hat{\boldsymbol{\theta}}_{\boldsymbol{B}i}\right\|\boldsymbol{s}_i^{\mathrm{T}}\,\mathrm{sgn}(\boldsymbol{s}_i)\right), \tag{24}$$

with the translational base frame adaptive law:

$$\dot{\hat{\boldsymbol{\theta}}}_{\boldsymbol{B}i}=\kappa\boldsymbol{Y}_k^{\mathrm{T}}\boldsymbol{E}_i-\kappa\boldsymbol{Y}_{\mathrm{b}}^{\mathrm{T}}\dot{\boldsymbol{e}}_{\mathrm{s}i}\boldsymbol{s}_i^{\mathrm{T}}\,\mathrm{sgn}(\boldsymbol{s}_i), \tag{25}$$

where η and κ are positive constants.

Theorem 1 Consider a cooperative manipulator system (5) with Assumptions 1–5. Together with the adaptive update laws (24) and (25), and the control robustness, the estimation error $\tilde{\boldsymbol{\Theta}}_i$ can be uniformly bounded ultimately, as $\tilde{\boldsymbol{\theta}}_{\boldsymbol{B}i}$ and ς_i can. The controller (21) guarantees the ultimate uniform boundedness of $\boldsymbol{s}_i$, the asymptotic stability of $\boldsymbol{e}_i$ and $\boldsymbol{e}_{\mathrm{s}i}$, and the desired value of $\boldsymbol{x}$.

Proof Consider the Lyapunov function candidate $V=\sum_{i=1}^{m}V_i$, where

$$V_i=\frac{1}{2}\boldsymbol{s}_i^{\mathrm{T}}\widehat{\boldsymbol{D}}_i\boldsymbol{s}_i+\frac{1}{2\eta}\tilde{\boldsymbol{\Theta}}_i^{\mathrm{T}}\tilde{\boldsymbol{\Theta}}_i+\frac{1}{2\kappa}\tilde{\boldsymbol{\theta}}_{\boldsymbol{B}i}^{\mathrm{T}}\tilde{\boldsymbol{\theta}}_{\boldsymbol{B}i}+\frac{1}{2}\varsigma_i^{\mathrm{T}}(\alpha\boldsymbol{K}_{\mathrm{V}}+\boldsymbol{K}_{\mathrm{P}})\varsigma_i, \tag{26}$$

V_i and V are all nonnegative scalars, and the derivative of Eq. (26) becomes

$$\dot{V}_i=\frac{1}{2}\boldsymbol{s}_i^{\mathrm{T}}\dot{\widehat{\boldsymbol{D}}}_i\boldsymbol{s}_i+\boldsymbol{s}_i^{\mathrm{T}}\widehat{\boldsymbol{D}}_i\dot{\boldsymbol{s}}_i+\frac{1}{\eta}\tilde{\boldsymbol{\Theta}}_i^{\mathrm{T}}\dot{\tilde{\boldsymbol{\Theta}}}_i+\frac{1}{\kappa}\tilde{\boldsymbol{\theta}}_{\boldsymbol{B}i}^{\mathrm{T}}\dot{\tilde{\boldsymbol{\theta}}}_{\boldsymbol{B}i}+\varsigma_i^{\mathrm{T}}(\alpha\boldsymbol{K}_{\mathrm{V}}+\boldsymbol{K}_{\mathrm{P}})\dot{\varsigma}_i. \tag{27}$$

Substituting Eqs. (19), (24), and (25) into Eq. (27), and using Eq. (21), we have

$$\begin{aligned}\dot{V}_i=&\boldsymbol{s}_i^{\mathrm{T}}\left(\frac{1}{2}\dot{\widehat{\boldsymbol{D}}}_i-\widehat{\boldsymbol{C}}_i\right)\boldsymbol{s}_i+\left(-\boldsymbol{s}_i^{\mathrm{T}}\hat{\boldsymbol{J}}_i^{\mathrm{T}}-\beta\dot{\boldsymbol{e}}_{\mathrm{s}i}^{\mathrm{T}}-\tilde{\boldsymbol{\theta}}_{\boldsymbol{B}}^{\mathrm{T}}\boldsymbol{Y}_{\mathrm{k}i}^{\mathrm{T}}\right)\boldsymbol{E}_i\\&+\varsigma_i^{\mathrm{T}}(\alpha\boldsymbol{K}_{\mathrm{V}}+\boldsymbol{K}_{\mathrm{P}})\dot{\varsigma}_i+\boldsymbol{s}_i^{\mathrm{T}}\left(\boldsymbol{\tau}_{\boldsymbol{d}_i}-\boldsymbol{\varepsilon}_i\right)\\&+\boldsymbol{s}_i^{\mathrm{T}}\left(-b_1\left\|\boldsymbol{s}_i^{\mathrm{T}}\right\|\mathrm{sgn}(\boldsymbol{s}_i)\right)+\tilde{\boldsymbol{\theta}}_{\boldsymbol{B}i}^{\mathrm{T}}\boldsymbol{Y}_{\mathrm{b}}^{\mathrm{T}}\dot{\boldsymbol{e}}_{\mathrm{s}i}(\boldsymbol{s}_i^{\mathrm{T}}\,\mathrm{sgn}(\boldsymbol{s}_i))\\&+\tilde{\boldsymbol{\Theta}}_i^{\mathrm{T}}\left(\left\|\boldsymbol{s}_i^{\mathrm{T}}\right\|\hat{\boldsymbol{\Theta}}_i+\left\|\hat{\boldsymbol{\theta}}_{\boldsymbol{B}i}\right\|\boldsymbol{s}_i^{\mathrm{T}}\,\mathrm{sgn}(\boldsymbol{s}_i^{\mathrm{T}})\right)\\&+\boldsymbol{s}_i^{\mathrm{T}}\left(-b_0\left\|\hat{\boldsymbol{\Theta}}_i\right\|_{\mathrm{F}}\left\|\boldsymbol{Y}_{\mathrm{b}}^{\mathrm{T}}\dot{\boldsymbol{e}}_{\mathrm{s}i}\right\|\mathrm{sgn}(\boldsymbol{s}_i)\right)\\=&\dot{V}_i^1+\dot{V}_i^2+\dot{V}_i^3+\dot{V}_i^4,\end{aligned} \tag{28}$$

where

$$\dot{V}_i^1=\boldsymbol{s}_i^{\mathrm{T}}\left(\frac{1}{2}\dot{\widehat{\boldsymbol{D}}}_i-\widehat{\boldsymbol{C}}_i\right)\boldsymbol{s}_i,$$

$$\begin{aligned}\dot{V}_i^2=&\left(-\boldsymbol{s}_i^{\mathrm{T}}\hat{\boldsymbol{J}}_i^{\mathrm{T}}-\beta\dot{\boldsymbol{e}}_{\mathrm{s}i}^{\mathrm{T}}-\beta\boldsymbol{K}_1\boldsymbol{e}^{\mathrm{T}}-\tilde{\boldsymbol{\theta}}_{\boldsymbol{B}i}^{\mathrm{T}}\boldsymbol{Y}_{\mathrm{k}}^{\mathrm{T}}\right)\boldsymbol{E}_i\\&+\varsigma_i^{\mathrm{T}}(\alpha\boldsymbol{K}_{\mathrm{V}}+\boldsymbol{K}_{\mathrm{P}})\dot{\varsigma}_i,\end{aligned} \tag{29}$$

$$\begin{aligned}\dot{V}_i^3=&\boldsymbol{s}_i^{\mathrm{T}}\left(\boldsymbol{\tau}_{\boldsymbol{d}_i}-\boldsymbol{\varepsilon}_i\right)+\boldsymbol{s}_i^{\mathrm{T}}\left(-b_1\left\|\boldsymbol{s}_i^{\mathrm{T}}\right\|\mathrm{sgn}(\boldsymbol{s}_i)\right)\\&+\tilde{\boldsymbol{\Theta}}_i^{\mathrm{T}}\left(\left\|\boldsymbol{s}_i^{\mathrm{T}}\right\|\hat{\boldsymbol{\Theta}}_i+\left\|\hat{\boldsymbol{\theta}}_{\boldsymbol{B}i}\right\|\boldsymbol{s}_i^{\mathrm{T}}\,\mathrm{sgn}(\boldsymbol{s}_i^{\mathrm{T}})\right),\end{aligned} \tag{30}$$

$$\begin{aligned}\dot{V}_i^4=&\tilde{\boldsymbol{\theta}}_{\boldsymbol{B}i}^{\mathrm{T}}\boldsymbol{Y}_{\mathrm{b}}^{\mathrm{T}}\dot{\boldsymbol{e}}_{\mathrm{s}i}(\boldsymbol{s}_i^{\mathrm{T}}\,\mathrm{sgn}(\boldsymbol{s}_i))\\&+\boldsymbol{s}_i^{\mathrm{T}}\left(-b_0\left\|\hat{\boldsymbol{\Theta}}_i\right\|_{\mathrm{F}}\left\|\boldsymbol{Y}_i^{\mathrm{T}}\dot{\boldsymbol{e}}_{\mathrm{s}i}\right\|\mathrm{sgn}(\boldsymbol{s}_i)\right).\end{aligned} \tag{31}$$

Considering Property 1 and time-independent matrix $\boldsymbol{\varpi}_i$, we can infer that

$$\dot{V}_i^1=\boldsymbol{s}_i^{\mathrm{T}}\left(\frac{1}{2}\dot{\widehat{\boldsymbol{D}}}_i-\widehat{\boldsymbol{C}}_i\right)\boldsymbol{s}_i=\boldsymbol{s}_i^{\mathrm{T}}\left(\frac{1}{2}\dot{\boldsymbol{\varpi}}_i\boldsymbol{J}_i^{\mathrm{T}}\boldsymbol{M}_{\mathrm{o}}(\boldsymbol{x})\boldsymbol{J}_i\right)\boldsymbol{s}_i=0. \tag{32}$$

From Eqs. (14) and (15), we find that

$$\boldsymbol{s}_{\mathrm{p}i}=\dot{\boldsymbol{x}}-\boldsymbol{Y}_{\mathrm{k}i}(\overline{\boldsymbol{q}}_i,\dot{\overline{\boldsymbol{q}}}_i)\tilde{\boldsymbol{\theta}}_{\boldsymbol{B}i}-\dot{\boldsymbol{x}}_{\mathrm{d}}+\alpha\varsigma_i=\dot{\boldsymbol{e}}_i-\boldsymbol{Y}_{\mathrm{k}i}\tilde{\boldsymbol{\theta}}_{\boldsymbol{B}i}+\alpha\varsigma_i. \tag{33}$$

Thus,

$$\begin{aligned}\dot{V}_i^2=&\left(-\boldsymbol{s}_i^{\mathrm{T}}\hat{\boldsymbol{J}}_i^{\mathrm{T}}-\beta\dot{\boldsymbol{e}}_{\mathrm{s}i}^{\mathrm{T}}-\beta\boldsymbol{K}_1\boldsymbol{e}^{\mathrm{T}}-\tilde{\boldsymbol{\theta}}_{\boldsymbol{B}i}^{\mathrm{T}}\boldsymbol{Y}_{\mathrm{k}i}^{\mathrm{T}}\right)\boldsymbol{E}_i\\&+\varsigma_i^{\mathrm{T}}(\alpha\boldsymbol{K}_{\mathrm{V}}+\boldsymbol{K}_{\mathrm{P}})\dot{\varsigma}_i\\=&\left(-\dot{\varsigma}_i-\alpha\varsigma_i\right)^{\mathrm{T}}\left(\boldsymbol{K}_{\mathrm{V}}\dot{\varsigma}_i+\boldsymbol{K}_{\mathrm{P}}\dot{\varsigma}_i\right)+\dot{\varsigma}_i^{\mathrm{T}}(\alpha\boldsymbol{K}_{\mathrm{V}}+\boldsymbol{K}_{\mathrm{P}})\dot{\varsigma}_i\\=&-\dot{\varsigma}_i^{\mathrm{T}}\boldsymbol{K}_{\mathrm{V}}\dot{\varsigma}_i-\alpha\dot{\varsigma}_i^{\mathrm{T}}\boldsymbol{K}_{\mathrm{P}}\dot{\varsigma}_i.\end{aligned} \tag{34}$$

Because $\boldsymbol{K}_{\mathrm{V}}$ and $\boldsymbol{K}_{\mathrm{P}}$ are all positive-definite diagonal, it is easy to see that $\dot{V}_i^2\le 0$. The ideal NN weights are bounded so that $\left\|\boldsymbol{\Theta}_i\right\|_{\mathrm{F}}\le\Theta_{\mathrm{M}}$ with known Θ_{M}. Similar to Lewis et al. (1998), we find that with positive constants a_0, a_1, and a_2, $\boldsymbol{s}_i^{\mathrm{T}}(\boldsymbol{\tau}_{\boldsymbol{d}_i}-\boldsymbol{\varepsilon}_i)\le\left\|\boldsymbol{s}_i^{\mathrm{T}}\right\|\left(a_0+a_1\left\|\tilde{\boldsymbol{\Theta}}_i\right\|_{\mathrm{F}}+a_2\left\|\boldsymbol{s}_i\right\|\left\|\tilde{\boldsymbol{\Theta}}_i\right\|_{\mathrm{F}}\right)$. We can also infer that $\mathrm{tr}(\tilde{\boldsymbol{\Theta}}_i^{\mathrm{T}}\hat{\boldsymbol{\Theta}}_i)=\mathrm{tr}(\tilde{\boldsymbol{\Theta}}_i^{\mathrm{T}}(\boldsymbol{\Theta}_i-\tilde{\boldsymbol{\Theta}}_i))\le\left\|\tilde{\boldsymbol{\Theta}}_i\right\|_{\mathrm{F}}\Theta_{\mathrm{M}}-\left\|\tilde{\boldsymbol{\Theta}}_i\right\|_{\mathrm{F}}^2$; hence,

$$\begin{aligned}\dot{V}_i^3=&\boldsymbol{s}_i^{\mathrm{T}}\left(\boldsymbol{\tau}_{\boldsymbol{d}_i}-\boldsymbol{\varepsilon}_i\right)+\boldsymbol{s}_i^{\mathrm{T}}\left(-b_1\left\|\boldsymbol{s}_i^{\mathrm{T}}\right\|\mathrm{sgn}(\boldsymbol{s}_i)\right)\\&+\tilde{\boldsymbol{\Theta}}_i^{\mathrm{T}}\left(\left\|\boldsymbol{s}_i^{\mathrm{T}}\right\|\hat{\boldsymbol{\Theta}}_i+\left\|\hat{\boldsymbol{\theta}}_{\boldsymbol{B}i}\right\|\boldsymbol{s}_i^{\mathrm{T}}\,\mathrm{sgn}(\boldsymbol{s}_i^{\mathrm{T}})\right)\\\le&\left\|\boldsymbol{s}_i^{\mathrm{T}}\right\|\Big(a_0+a_1\left\|\tilde{\boldsymbol{\Theta}}_i\right\|_{\mathrm{F}}+a_2\left\|\boldsymbol{s}_i\right\|\left\|\tilde{\boldsymbol{\Theta}}_i\right\|_{\mathrm{F}}-b_1\boldsymbol{s}_i^{\mathrm{T}}\,\mathrm{sgn}(\boldsymbol{s}_i)\\&+\left\|\tilde{\boldsymbol{\Theta}}_i\right\|_{\mathrm{F}}\Theta_{\mathrm{M}}-\left\|\tilde{\boldsymbol{\Theta}}_i\right\|_{\mathrm{F}}^2+\left\|\tilde{\boldsymbol{\Theta}}_i\right\|_{\mathrm{F}}\left\|\hat{\boldsymbol{\theta}}_{\boldsymbol{B}i}\right\|\Big)\\=&\left\|\boldsymbol{s}_i^{\mathrm{T}}\right\|\Big[-\left\|\tilde{\boldsymbol{\Theta}}_i\right\|_{\mathrm{F}}^2+\Big(a_1+a_2\left\|\boldsymbol{s}_i\right\|+\Theta_{\mathrm{M}}\\&+\left\|\hat{\boldsymbol{\theta}}_{\boldsymbol{B}i}\right\|\Big)\left\|\tilde{\boldsymbol{\Theta}}_i\right\|_{\mathrm{F}}+a_0-b_1\boldsymbol{s}_i^{\mathrm{T}}\,\mathrm{sgn}(\boldsymbol{s}_i)\Big].\end{aligned} \tag{35}$$

Let $\gamma_i = a_1 + a_2\|\boldsymbol{s}_i\| + \Theta_{\mathrm{M}} + \|\hat{\boldsymbol{\theta}}_{\boldsymbol{B}i}\|$. Then

$$\begin{aligned}\dot{V}_i^3 &= \|\boldsymbol{s}_i^{\mathrm{T}}\|\left(-\|\tilde{\boldsymbol{\Theta}}_i\|_{\mathrm{F}}^2 + \gamma_i\|\tilde{\boldsymbol{\Theta}}_i\|_{\mathrm{F}} + a_0 - b_1\boldsymbol{s}_i^{\mathrm{T}}\operatorname{sgn}(\boldsymbol{s}_i)\right)\\ &= \|\boldsymbol{s}_i^{\mathrm{T}}\|\left[-\left(\|\tilde{\boldsymbol{\Theta}}_i\|_{\mathrm{F}} - \frac{\gamma_i}{2}\right)^2 + \frac{\gamma_i^2}{4} + a_0 - b_1\boldsymbol{s}_i^{\mathrm{T}}\operatorname{sgn}(\boldsymbol{s}_i)\right].\end{aligned}$$

Thus, $\dot{V}_{3i} \le 0$ as long as

$$\|\tilde{\boldsymbol{\Theta}}_i\|_{\mathrm{F}} \ge \frac{\gamma_i}{2} + \sqrt{\frac{\gamma_i^2}{4} + a_0}, \tag{36}$$

or

$$\|\boldsymbol{s}_i\| \ge \boldsymbol{s}_i^{\mathrm{T}}\operatorname{sgn}(\boldsymbol{s}_i) \ge \frac{\left(a_1 + \Theta_{\mathrm{M}} + \|\hat{\boldsymbol{\theta}}_{\boldsymbol{B}i}\|\right)\|\tilde{\boldsymbol{\Theta}}_i\|_{\mathrm{F}} + a_0}{b_1 - a_2\|\tilde{\boldsymbol{\Theta}}_i\|_{\mathrm{F}}}, \tag{37}$$

where $b_1 - a_2\|\tilde{\boldsymbol{\Theta}}_i\|_{\mathrm{F}} > 0$. Select proper parameters leading to $b_0 \ge \theta_{\mathrm{B}}^{\mathrm{M}} / \|\hat{\boldsymbol{\Theta}}_i\|_{\mathrm{F}}$; hence,

$$\begin{aligned}\dot{V}_i^4 &= \boldsymbol{s}_i^{\mathrm{T}}\left(-b_0\|\hat{\boldsymbol{\Theta}}_i\|_{\mathrm{F}}\|\boldsymbol{Y}_{\mathrm{b}}^{\mathrm{T}}\dot{\boldsymbol{e}}_{\mathrm{s}i}\|\operatorname{sgn}(\boldsymbol{s}_i)\right)\\ &\quad + \tilde{\boldsymbol{\theta}}_{\boldsymbol{B}i}^{\mathrm{T}}\boldsymbol{Y}_{\mathrm{b}}^{\mathrm{T}}\dot{\boldsymbol{e}}_{\mathrm{s}i}(\boldsymbol{s}_i^{\mathrm{T}}\operatorname{sgn}(\boldsymbol{s}_i)) \le 0.\end{aligned} \tag{38}$$

Therefore, $\dot{V}_i = \sum_{j=1}^4 \dot{V}_i^j \le 0$ and it is negative outside a compact set, $\hat{\boldsymbol{D}}_i$ is uniformly positive definite (PDT), and V_i is PDT with $\boldsymbol{s}_i$, $\tilde{\boldsymbol{\Theta}}_i$, $\tilde{\boldsymbol{\theta}}_{\boldsymbol{B}i}$, ς_i. Because $\dot{V}_i \le 0$, V_i is bounded, $\boldsymbol{s}_i$, $\tilde{\boldsymbol{\Theta}}_i$, $\tilde{\boldsymbol{\theta}}_{\boldsymbol{B}i}$, ς_i are all bounded, $\hat{\boldsymbol{\Theta}}_i$ and $\tilde{\boldsymbol{\theta}}_{\boldsymbol{B}i}$ are bounded, and $\boldsymbol{s}_{xi}$ is bounded as from Eq. (16). From Eq. (13) we find that ς_i is linear with $\boldsymbol{e}_i$ and $\boldsymbol{e}_{\mathrm{s}i}$. $\boldsymbol{e}_i$ and $\boldsymbol{e}_{\mathrm{s}i}$ are also bounded, and $\boldsymbol{x}$ is bounded if $\boldsymbol{x}_{\mathrm{d}}$ is bounded, and $\dot{\boldsymbol{x}}_{\mathrm{r}i}$ is bounded if $\dot{\boldsymbol{x}}_{\mathrm{d}}$ is bounded. Therefore, $\dot{\boldsymbol{q}}_{\mathrm{r}i}$ is bounded from Eq. (16), with bounded $\hat{\boldsymbol{J}}_i^+$; that is, $\hat{\boldsymbol{J}}_i$ is of full rank and is bounded. Because $\boldsymbol{s}_i = \dot{\boldsymbol{q}}_i - \dot{\boldsymbol{q}}_{\mathrm{r}i}$ is bounded, $\dot{\boldsymbol{q}}_i$ is bounded, and $\dot{\boldsymbol{x}}$ is bounded with a bounded Jacobian matrix. Thus, $\dot{\boldsymbol{e}}_i$ is bounded, so is $\dot{\boldsymbol{e}}_{\mathrm{s}i}$, and $\ddot{\boldsymbol{x}}_{\mathrm{r}i}$ is bounded with bounded $\ddot{\boldsymbol{x}}_{\mathrm{d}}$. Therefore, $\dot{\varsigma}_i = \dot{\boldsymbol{e}}_i + \beta\dot{\boldsymbol{e}}_{\mathrm{s}i}$ is bounded. From Barbalat's lemma, $\boldsymbol{e}_i$, $\boldsymbol{e}_{\mathrm{s}i}$, and ς_i are all uniformly continuous, which means that $\lim_{t\to\infty}\boldsymbol{e}_i = \boldsymbol{0}$ and $\lim_{t\to\infty}\boldsymbol{e}_{\mathrm{s}i} = \boldsymbol{0}$. As $t \to 0$, the controller guarantees the asymptotic stability of the tracking errors $\boldsymbol{e}_i$ and $\boldsymbol{e}_{\mathrm{s}i}$. Thus, $\boldsymbol{x}$ is guaranteed to be their desired values.

The uniform ultimate boundedness of $\|\boldsymbol{s}_i\|$ and $\|\tilde{\boldsymbol{\Theta}}_i\|_{\mathrm{F}}$ is proved according to the Lyapunov theorem extension (Lewis et al., 1998). The uniform ultimate boundedness of $\boldsymbol{s}_i$ is guaranteed. From Eq. (28), error $\|\boldsymbol{s}_i\|$ can be slightly adjusted arbitrarily by increasing the result of $\left(b_1 - a_2\|\tilde{\boldsymbol{\Theta}}_i\|_{\mathrm{F}}\right)$ and decreasing the result of $\left(a_1 + \Theta_{\mathrm{M}} + \|\hat{\boldsymbol{\theta}}_{\boldsymbol{B}i}\|\right)\|\tilde{\boldsymbol{\Theta}}_i\|_{\mathrm{F}} + a_0$.

4 Simulation and discussion

4.1 Simulation settings

To illustrate the performance of the adaptive tracking controller, numerical studies are presented in this subsection. The two planar three-degree-of-freedom (3-DOF) robotic manipulators' dynamics is similar to that in Zribi et al. (2000), and they hold a common circular disc rigidly. The object model is expressed as

$$\begin{bmatrix} m_{\mathrm{o}} & 0 & 0\\ 0 & m_{\mathrm{o}} & 0\\ 0 & 0 & I_{\mathrm{o}}\end{bmatrix}\begin{bmatrix} x\\ y\\ R\end{bmatrix} + \begin{bmatrix} 0\\ m_{\mathrm{o}}g\\ 0\end{bmatrix} = \begin{bmatrix} F_{\mathrm{o}x}\\ F_{\mathrm{o}y}\\ F_{\mathrm{o}z}\end{bmatrix},$$

where m_{o}=1.5 kg is the mass of the circular disc, rotational inertia I_{o}=0.3 kg·m^2, gravitational acceleration g=9.8 N/kg, and the circular radius is 0.2 m. (x, y, R) represent the center and angle of the disc diameter contact points, joining with the world frame axis separately. The stiffness is assumed to be 300 kN/m only for computing force during simulation.

Uncertain kinematic parameters are given as $\hat{\boldsymbol{\theta}}_{\boldsymbol{B}i} = [\hat{\boldsymbol{B}}_i;\ \boldsymbol{\theta}_{\mathrm{k}i}] = [\hat{\boldsymbol{B}}_i;\ l_1;\ l_2;\ l_3;\ 1;\ 1;\ 1;\ 1]$, where l_1, l_2, and l_3 denote the link length of manipulators as 0.6, 0.6, and 0.2 m, respectively. The bases of the two manipulators are set to (B_{1x}, B_{1y})=(−0.4, 0) and (B_{2x}, B_{2y})=(0.4, 0) in reality, with inaccurate $(\hat{B}_{1x},\ \hat{B}_{1y}) =$ (−0.39, 0.01) and $(\hat{B}_{2x},\ \hat{B}_{2y}) = (0.39,\ 0)$ for nominal known (regarded as calibration error) with controller design. Thus, the relative base frame parameters are (0.8, 0) in reality, with (0.78, 0.01) for initialization as inaccurate translational parameters in both vertical and horizontal dimensions.

Joint friction is introduced as $\boldsymbol{\tau}_{\mathrm{f}_i}(\dot{\boldsymbol{q}}_i)=$ diag(0.15, 0.05, 0.01)$\dot{\boldsymbol{q}}_i$+diag(0.02, 0.01, 0.005)sgn($\dot{\boldsymbol{q}}_i$), and the external disturbance $\boldsymbol{d}_i(t)$=[0.1, 0.1, 0.04]$^{\mathrm{T}}\cdot$ sin(0.2πt)+[0.2, 0.2, 0.1]$^{\mathrm{T}}$. The initial values for object motion are set as $x(0)$=0.2, $y(0)$=0.8, $R(0)$=0, $\dot{x}(0)=0$, $\dot{y}(0)=0$, $\dot{R}(0)=0$. The desired trajectory for the circular disc is a circle described as X_{d}= 0.2cos(0.2πt), Y_{d}=0.2sin(0.2πt)+0.8, and the disc is always held steady horizontally with zero rotation and without any internal force. The simulation time is set as 15 s at a frequency of 250 Hz.

4.2 Simulation results

To address the effectiveness of the proposed approach with practical consideration, together with the proposed ANNR, three controllers are adopted and compared in simulation. A traditional proportional-integral-derivative (PID) controller is

$$\boldsymbol{\tau}_i=\boldsymbol{K}_{\mathrm{P}}\tilde{\boldsymbol{q}}_i+\boldsymbol{K}_{\mathrm{I}}\int\tilde{\boldsymbol{q}}_i\mathrm{d}t+\boldsymbol{K}_{\mathrm{D}}\dot{\tilde{\boldsymbol{q}}}_i, \tag{39}$$

and an efficient robust control (ERC) method is

$$\boldsymbol{\tau}_i=-\boldsymbol{K}_{d_i}\boldsymbol{s}_{r_i}-\boldsymbol{J}_{\phi_i}^{\mathrm{T}}(\boldsymbol{q}_i)(\boldsymbol{f}_{d_i}-\boldsymbol{K}_{f_i}\tilde{\boldsymbol{f}}_i), \tag{40}$$

where $\boldsymbol{s}_{r_i}-\alpha_i\boldsymbol{\sigma}_i=\boldsymbol{s}_i-\boldsymbol{s}_{d_i}=\boldsymbol{s}_{q_i}$, $\boldsymbol{s}_{d_i}=\boldsymbol{s}_i(t_0)\mathrm{e}^{-k_i(t-t_0)}$, and $\boldsymbol{s}_i=\hat{\boldsymbol{J}}^{+}(\boldsymbol{q}_i)(\dot{\tilde{\boldsymbol{x}}}+\gamma_i\tilde{\boldsymbol{x}})$. Details can be found in Gueaieb et al. (2007a) for ERC. The following parameter values are taken: (1) For PID, inverse kinematic is adopted with an inaccurate translational base frame, and $\boldsymbol{K}_{\mathrm{P}}$=3000, $\boldsymbol{K}_{\mathrm{D}}$=80, and $\boldsymbol{K}_{\mathrm{I}}$=190; (2) For ERC, inverse kinematic is adopted with an inaccurate translational base frame, and $\boldsymbol{K}_{f_i}=0$, $\boldsymbol{K}_{d_i}=2$, α_i=10, γ_i=diag(70, 70, 70), and k_i=5; (3) For ANNR, zero inverse kinematic calculation is adopted, and $\boldsymbol{K}_{\mathrm{I}}$=diag(0.005, 0.005, 0.005), $\boldsymbol{K}_{\mathrm{V}}$=diag(80, 80, 20), $\boldsymbol{K}_{\mathrm{P}}$=diag(8000, 8000, 3000), α=0.1, κ=0.05, b_0=0.1, b_1=0.5, $\varpi_1=\varpi_2=0.5$, and β=0.5. An NN has 27 inputs, five hidden RBFs, and three outputs for each, b=0.2 and η=0.2 for learning weight, and

$$\boldsymbol{Y}_{\mathrm{b}}=\begin{bmatrix}1200&0&0&0&0&0&0&0&0\\0&120&0&0&0&0&0&0&0\\0&0&0&0&0&0&0&0&0\end{bmatrix}.$$

Considering the ranges of the NN inputs, the centers of Gaussian functions are chosen as $\boldsymbol{c}$=[−0.5, −0.25, 0, 0.25, 0.5; −0.5, −0.25, 0, 0.25, 0.5; −0.5, −0.25, 0, 0.25, 0.5; −0.2, −0.1, 0, 0.1, 0.2; −0.2, −0.1, 0, 0.1, 0.2; −0.2, −0.1, 0, 0.1, 0.2; −0.2, −0.1, 0, 0.1, 0.2; −1, −0.5, 0, 0.5, 1; −0.1, −0.05, 0, 0.05, 0.1; −0.2, −0.1, 0, 0.1, 0.2; −0.2, −0.1, 0, 0.1, 0.2; −0.1, −0.05, 0, 0.05, 0.1; −0.1, −0.05, 0, 0.05, 0.1; −0.1, −0.05, 0, 0.05, 0.1; −0.1, −0.05, 0, 0.05, 0.1; −0.1, −0.05, 0, 0.05, 0.1; −0.1, −0.05, 0, 0.05, 0.1; −0.1, −0.05, 0, 0.05, 0.1; −0.4, −0.2, 0, 0.2, 0.4; −0.6, −0.3, 0, 0.3, 0.6; −0.6, −0.3, 0, 0.3, 0.6; −0.4, −0.2, 0, 0.2, 0.4; −1, −0.5, 0, 0.5, 1; −1, −0.5, 0, 0.5, 1; −1, −0.5, 0, 0.5, 1; −1, −0.5, 0, 0.5, 1].

In the presence of inaccurate two-dimensional translational base parameters, joint frictions, and external disturbances, the object's global position and internal force tracking errors can be found in Fig. 2. Using the proposed ANNR, the translational tracking error (ΔX and ΔY) and rotational tracking error (ΔR) converge to zero within 2 s. Although ANNR shows little oscillation with ΔX, it converges faster and is more precise than the other two. PID is far more affected by those uncertainties than ANNR. The control performance using ERC is less satisfactory, because an obvious oscillation occurs (Fig. 2d). The results show excellent robustness within the proposed ANNR. In addition, internal force $\boldsymbol{f}_i$ remains small and steady using ANNR, whereas other controllers exhibit excessive or unstable internal forces in comparison. This illustrates that the proposed approach not only guarantees position error convergence but also makes it converge in a synchronous manner.

Little difference can be found within the joint angle (Fig. 3a). However, PID and ANNR provide smooth joint velocity plots, whereas the plots of ERC chatter. Note that inverse kinematics is essential for both PID and ERC, but not for the proposed ANNR. It is also important to note that, for traditional regressor matrix-based adaptive controllers (Cheah et al., 2006; Gueaieb et al., 2007b; Zhao et al., 2014a), the regressor matrix would become much more complex due to the increase of the number of manipulator

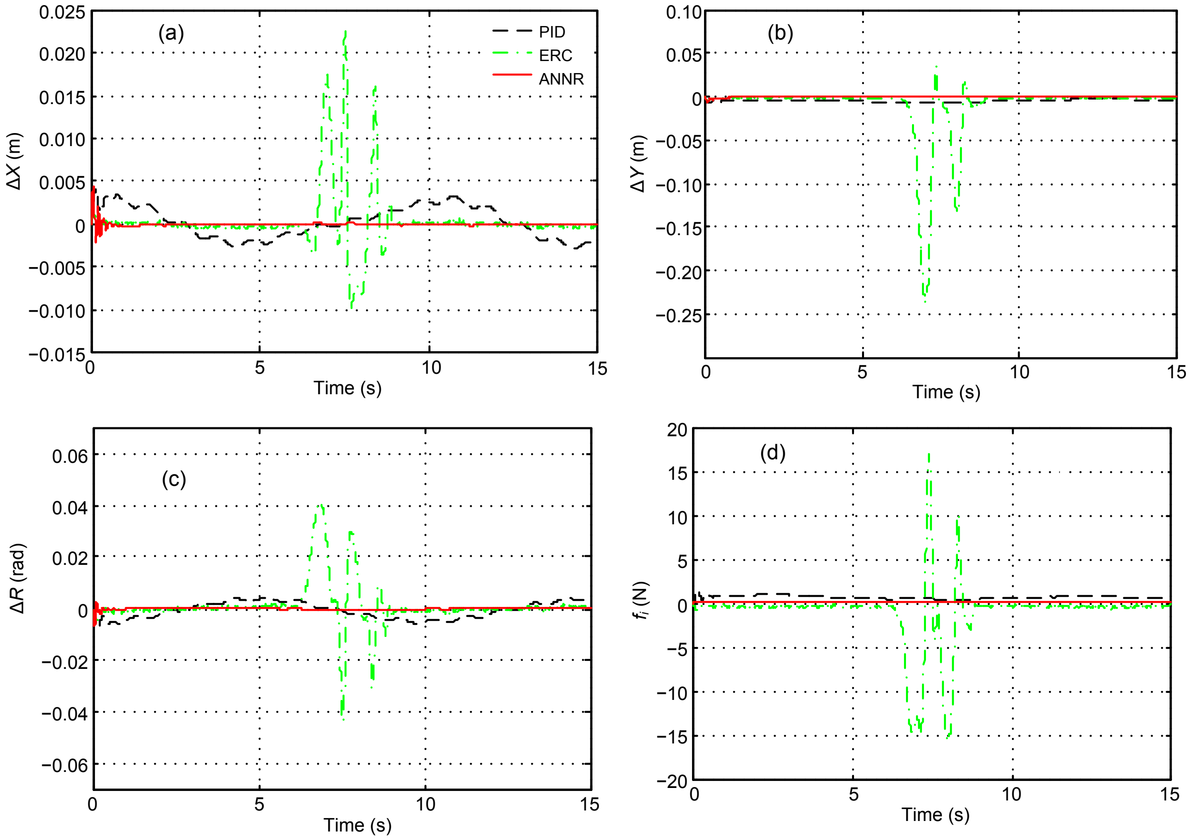

Fig. 2 Position and internal force tracking errors under a circular trajectory, with inaccurate translational base frame parameters, amplified friction, and external disturbances: (a) ΔX; (b) ΔY; (c) ΔR; (d) f_i

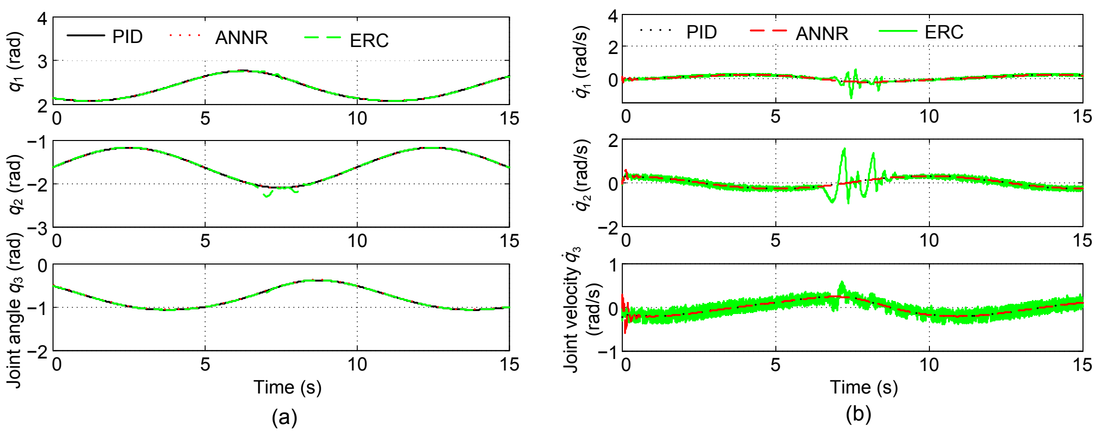

Fig. 3 Joint angle and velocity under a circular trajectory: (a) joint angle; (b) joint velocity

degrees and the number of the estimated parameters. Unlike those regressor matrix-based methods, the proposed ANNR avoids common dynamical regression with NN estimation. Only the kinematic regression is required.

To strengthen the verification, another test is established including another straight trajectory. The initial values for object motion are set with $x(0)=0$, $y(0)=0.6$, $R(0)=0$, $\dot{x}(0)=0$, $\dot{y}(0)=0$, and $\dot{R}(0)=0$. The desired straight trajectory is described as $X_{\mathrm{d}}=0$,

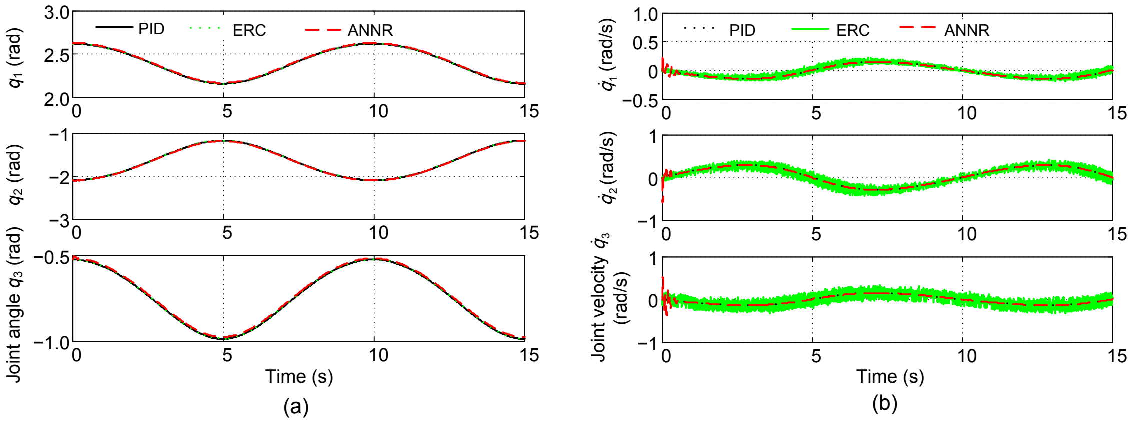

Fig. 4 Joint angle and velocity under a straight trajectory: (a) joint angle; (b) joint velocity

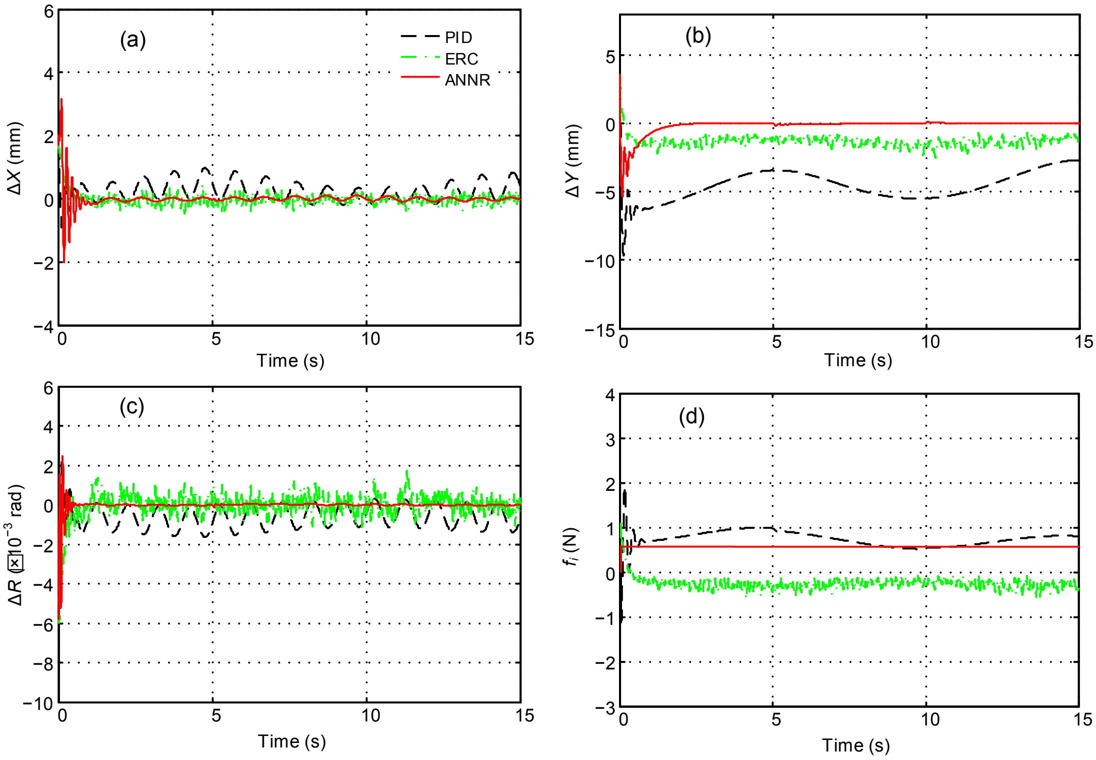

Fig. 5 Position and internal force tracking errors under a straight trajectory, with inaccurate translational base frame parameters, amplified friction, and external disturbances: (a) ΔX; (b) ΔY; (c) ΔR; (d) f_i

Y_d=0.8−0.2cos(0.2πt). All other parameters and weights are exactly the same as in the former circular trajectory simulation. In this case, we examine the joint angle and velocity (Fig. 4). Fig. 5 illustrates the object's task space tracking errors, where the proposed ANNR exhibits significant robustness against those inaccuracies and disturbances. In spite of insignificant internal force, an acceptable tracking accuracy can always be obtained, while the internal force can be reduced by weight tuning.

In the merit of system adaptation and neural estimation, the proposed ANNR can stabilize position tracking of each manipulator while adjusting its relative base frame parameters. Fig. 6 depicts the estimation of relative translational base frame parameters between the two cooperative manipulators, for both circular and straight trajectories. One can see that the proposed approach provides satisfactory self-tuning and estimation, especially in the circular trajectory, because we maintain the weight setting to the straight trajectory. This also illustrates the potential for accurate online calibration.

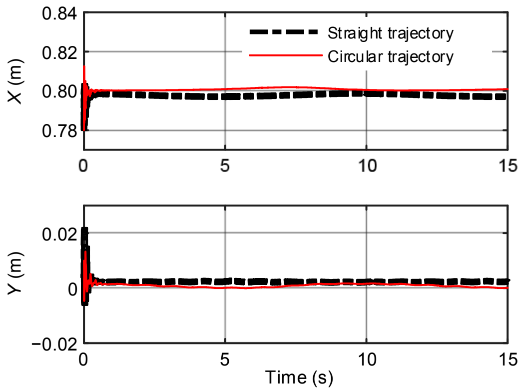

Fig. 6 Estimation of relative translational base frame parameters

5 Conclusions

By theoretical analysis and simulation demonstrations, a novel adaptive, robust neural controller has been constructed to cope with inaccurate translational base frame parameters, modeling uncertainty, unknown joint frictions, and external disturbances within cooperative manipulation. This controller has the following characteristics:

1. No prior knowledge of the system dynamics is required. The adopted RBF NN estimation performs well despite uncertain modeling, joint frictions, external disturbances, and more importantly, the internal force. Inaccurate translational base frame parameters can be calibrated online to achieve a satisfactory accuracy with another adaptive engine.

2. Besides NN estimation, robustness is achieved with an additional robust control procedure that could cope with dynamic and kinematic estimation errors.

3. The proposed approach guarantees that both the global tracking error and the synchronization error converge to 0 asymptotically and simultaneously, and keeps the internal force in an acceptable range steadily.

The overall stability is proved through a Lyapunov function and simulations. The controller is also feasible for cooperative systems with more than two manipulators, but will need some redesign to accommodate an appropriate estimated synchronization function to cover all manipulators. Orientation inaccuracy may be considered, but first with another compact rearrangement of forward kinematics as in Figs. 4 and 5, because accurate access to kinematic regression matrices would no longer be obtained. Because we pay attention to translational inaccuracy here and more issues may occur with other kinds of base frame error, future work may focus on situations with more complicated inaccurate base frame parameters. NNs with various network topologies, different numbers of neurons, layers, or activation functions may work here, but not with respect to our main concern, which is also taken as a future scope of research.

References

Aghili F, 2011. Self-tuning cooperative control of manipulators with position/orientation uncertainties in the closed-kinematic loop. IEEE/RSJ Int Conf on Intelligent Robots and Systems, p.4187-4193. https://doi.org/10.1109/IROS.2011.6094470

Aghili F, 2013. Adaptive control of manipulators forming closed kinematic chain with inaccurate kinematic model. *IEEE/ASME Trans Mechatron*, 18(5):1544-1554. https://doi.org/10.1109/tmech.2012.2207964

Cheah CC, Liu C, Slotine J, 2004. Approximate Jacobian adaptive control for robot manipulators. IEEE Int Conf on Robtics and Automation, p.3075-3080. https://doi.org/10.1109/ROBOT.2004.1307529

Cheah CC, Liu C, Slotine JJE, 2006. Adaptive Jacobian tracking control of robots with uncertainties in kinematic, dynamic and actuator models. *IEEE Trans Autom Contr*, 51(6):1024-1029. https://doi.org/10.1109/TAC.2006.876943

Cheng L, Hou ZG, Tan M, 2009. Adaptive neural network tracking control for manipulators with uncertain kinematics, dynamics and actuator model. *Automatica*, 45(10):2312-2318. https://doi.org/10.1016/j.automatica.2009.06.007

Corke P, 1996. A robotics toolbox for Matlab. *IEEE Robot Autom Mag*, 3(1):24-32. https://doi.org/10.1109/100.486658

Deng H, Wu H, Yang C, et al., 2015. Base frame calibration for multi-robot coordinated systems. IEEE Int Conf on Robotics and Biomimetics, p.1489-1494. https://doi.org/10.1109/ROBIO.2015.7418981

Erhart S, Hirche S, 2013. Adaptive force/velocity control for multi-robot cooperative manipulation under uncertain kinematic parameters. IEEE/RSJ Int Conf on Intelligent Robots and Systems, p.307-314. https://doi.org/10.1109/IROS.2013.6696369

Gan Y, Dai X., 2011. Base frame calibration for coordinated industrial robots. *Robot Auton Syst*, 59(7-8):563-570. https://doi.org/10.1016/j.robot.2011.04.003

Gueaieb W, Al-Sharhan S, Bolic M, 2007a. Robust computationally efficient control of cooperative closed-chain manipulators with uncertain dynamics. *Automatica*, 43(5): 842-851. https://doi.org/10.1016/j.automatica.2006.10.025

Gueaieb W, Karray F, Al-Sharhan S, 2007b. A robust hybrid intelligent position/force control scheme for cooperative manipulators. *IEEE/ASME Trans Mechatron*, 12(2):109-125. https://doi.org/10.1109/TMECH.2007.892820

Lewis F, Jagannathan S, Yesildirak A, 1998. Neural Network Control of Robot Manipulators and Non-linear Systems. CRC Press, France, p.1-468.

Li Z, Xiao S, Ge SS, et al., 2015. Constrained multilegged robot system modeling and fuzzy control with uncertain kinematics and dynamics incorporating foot force optimization. *IEEE Trans Syst Man Cybern Syst*, 46(1):1-15. https://doi.org/10.1109/TSMC.2015.2422267

Liu JF, Abdel-Malek K, 2000. Robust control of planar dual-arm cooperative manipulators. *Robot Comput-Integr Manuf*, 16(2):109-119. https://doi.org/10.1016/S0736-5845(99)00043-5

Liu YC, 2015. Distributed synchronization for heterogeneous robots with uncertain kinematics and dynamics under switching topologies. *J Franklin Instit*, 352(9):3808-3826. https://doi.org/10.1016/j.jfranklin.2014.11.018

Liu YC, Khong MH, 2015. Adaptive control for nonlinear teleoperators with uncertain kinematics and dynamics. *IEEE/ASME Trans Mechatron*, 20(5):2550-2562. https://doi.org/10.1109/TMECH.2015.2388555

Lizarralde F, Leite AC, Hsu L, et al., 2013. Adaptive visual servoing scheme free of image velocity measurement for uncertain robot manipulators. *Automatica*, 49(5):1304-1309. https://doi.org/10.1016/j.automatica.2013.01.047

Mohajerpoor R, Rezaei M, Talebi A, et al., 2011. A robust adaptive hybrid force/position control scheme of two planar manipulators handling an unknown object interacting with an environment. *Proc Instit Mech Eng Part I J Syst Contr Eng*, 226(4):509-522. https://doi.org/10.1177/0959651811424251

Namvar M, Aghili F, 2005. Adaptive force-motion control of coordinated robots interacting with geometrically unknown environments. *IEEE Trans Robot*, 21(4):678-694. https://doi.org/10.1109/TRO.2004.842346

Panwar V, Kumar N, Sukavanam N, et al., 2012. Adaptive neural controller for cooperative multiple robot manipulator system manipulating a single rigid object. *Appl Soft Comput*, 12(1):216-227. https://doi.org/10.1016/j.asoc.2011.08.051

Park IW, Lee BJ, Cho SH, et al., 2012. Laser-based kinematic calibration of robot manipulator using differential kinematics. *IEEE/ASME Trans Mechatron*, 17(6):1059-1067. https://doi.org/10.1109/TMECH.2011.2158234

Park J, Sandberg IW, 1991. Universal approximation using radial-basis-function networks. *Neur Comput*, 3(2):246-257. https://doi.org/10.1162/neco.1991.3.2.246

Parra-Vega V, Arimoto S, Liu YH, et al., 2003. Dynamic sliding pid control for tracking of robot manipulators: theory and experiments. *IEEE Trans Robot Autom*, 19(6):967-976. https://doi.org/10.1109/TRA.2003.819600

Su CY, Stepanenko Y, 1995. Adaptive sliding mode coordinated control of multiple robot arms attached to a constrained object. *IEEE Trans Syst Man Cybern*, 25(5):871-878. https://doi.org/10.1109/21.376500

Szewczyk J, Plumet F, Bidaud P, 2002. Planning and controlling cooperating robots through distributed impedance. *J Robot Syst*, 19(6):283-297. https://doi.org/10.1002/rob.10041

Tavasoli A, Eghtesad M, Jafarian H, 2009. Two-time scale control and observer design for trajectory tracking of two cooperating robot manipulators moving a flexible beam. *Robot Auton Syst*, 57(2):212-221. https://doi.org/10.1016/j.robot.2008.04.003

Zhang YH, Wei W, Dan YU, et al., 2011. A tracking and predicting scheme for ping pong robot. *J Zhejiang Univ-Sci C (Comput & Electron)*, 12(2):110-115. https://doi.org/10.1631/jzus.C0910528

Zhao D, Li S, Zhu Q, 2014a. Adaptive synchronised tracking control for multiple robotic manipulators with uncertain kinematics and dynamics. *Int J Syst Sci*, 47(4):1-14. https://doi.org/10.1080/00207721.2014.906681

Zhao D, Ni W, Zhu Q, 2014b. A framework of neural networks based consensus control for multiple robotic manipulators. *Neurocomputing*, 140:8-18. https://doi.org/10.1016/j.neucom.2014.03.041

Zhao D, Zhu Q, Li N, et al., 2014c. Synchronized control with neuro-agents for leader–follower based multiple robotic manipulators. *Neurocomputing*, 124:149-161. https://doi.org/10.1016/j.neucom.2013.07.016

Zribi M, Karkoub M, Huang L, 2000. Modelling and control of two robotic manipulators handling a constrained object. *Appl Math Model*, 24(12):881-898. https://doi.org/10.1016/S0307-904X(00)00022-6